Provided for non-commercial research and education use.
Not for reproduction, distribution or commercial use.



This article appeared in a journal published by Elsevier. The attached copy is furnished to the author for internal non-commercial research and education use, including for instruction at the authors institution and sharing with colleagues.

Other uses, including reproduction and distribution, or selling or licensing copies, or posting to personal, institutional or third party websites are prohibited.

In most cases authors are permitted to post their version of the article (e.g. in Word or Tex form) to their personal website or institutional repository. Authors requiring further information regarding Elsevier's archiving and manuscript policies are encouraged to visit:

http://www.elsevier.com/copyright

Author's personal copy

International Communications in Heat and Mass Transfer 38 (2011) 218–228

Contents lists available at ScienceDirect

International Communications in Heat and Mass Transfer

journal homepage: www.elsevier.com/locate/ichmt

Numerical investigation on the single phase forced convection heat transfer characteristics of TiO_2 nanofluids in a double-tube counter flow heat exchanger ☆

H. Demir [a,*], A.S. Dalkilic [a], N.A. Kürekci [a], W. Duangthongsuk [b], S. Wongwises [b,*]

[a] Heat and Thermodynamics Division, Department of Mechanical Engineering, Yildiz Technical University (YTU), Yildiz, Besiktas, Istanbul 34349, Turkey
[b] Fluid Mechanics, Thermal Engineering and Multiphase Flow Research Lab. (FUTURE), Department of Mechanical Engineering, King Mongkut's University of Technology Thonburi (KMUTT), Bangmod, Bangkok 10140, Thailand

ARTICLE INFO

Available online 21 December 2010

Keywords:
Heat transfer coefficient
Pressure drop
Wall shear stress
Nanofluid
Heat exchanger

ABSTRACT

In this study, forced convection flows of nanofluids consisting of water with TiO_2 and Al_2O_3 nanoparticles in a horizontal tube with constant wall temperature are investigated numerically. The horizontal test section is modeled and solved using a CFD program. Palm et al.'s correlations are used to determine the nanofluid properties. A single-phase model having two-dimensional equations is employed with either constant or temperature dependent properties to study the hydrodynamics and thermal behaviors of the nanofluid flow. The numerical investigation is performed for a constant particle size of Al_2O_3 as a case study after the validation of its model by means of the experimental data of Duangthongsuk and Wongwises with TiO_2 nanoparticles. The velocity and temperature vectors are presented in the entrance and fully developed region. The variations of the fluid temperature, local heat transfer coefficient and pressure drop along tube length are shown in the paper. Effects of nanoparticles concentration and Reynolds number on the wall shear stress, Nusselt number, heat transfer coefficient and pressure drop are presented. Numerical results show the heat transfer enhancement due to presence of the nanoparticles in the fluid in accordance with the results of the experimental study used for the validation process of the numerical model.

© 2010 Elsevier Ltd. All rights reserved.

1. Introduction

Water, oil, and ethylene glycol mixture is one of the low thermal conductivity of widely used conventional heat transfer fluids that limits the enhancement of the performance and compactness of these devices belong to the electronic, automotive and aerospace industries. Improvements on the thermal conductivity by suspending small solid particles in the fluid are one of the solutions to prevent this disadvantage. Thermal conductivity is an important parameter in enhancing the heat transfer performance of a heat transfer fluid. Since the thermal conductivity of solid metals is higher than that of fluids, the suspended particles are expected to be able to increase the thermal conductivity and heat transfer performance. Many researchers have reported experimental studies on the thermal conductivity of nanofluids. Metallic, non-metallic and polymeric particles are used to form slurries by adding into fluids. Some of problems such as abrasion and clogging can be seen due to the suspended particles' sizes that are of millimeter dimensions. For that reason, these kinds of large particles are not suitable for heat transfer enhancement. Recently, advances in manufacturing technologies have made the production of particles in the nanometer scale possible (i.e., 10 nm<particle diameter<100 nm). The uniform and stable suspensions are obtained by means of these smaller sized particles. Thus, the nanofluids provide higher heat transfer enhancement than existing techniques. The use of particles of nanometer dimension was first continuously studied by a research group at the Argonne National Laboratory around a decade ago. Choi [1] was probably the first one who called the fluids with particles of nanometer dimensions 'nano-fluids'. The term 'nanofluid' refers to a two-phase mixture usually composed of a continuous liquid phase and dispersed nanoparticles in suspension.

In spite of the two phase mixture specialty of nanofluids, they are easily fluidized and can be nearly considered to behave as a fluid [2] due to the tiny size of solid particles. For that reason, it is possible for nanofluids to be treated as single phase flow. It is assumed that the fluid phase and particles are in thermal equilibrium and moving with the same velocity in certain conditions [3] considering the ultrafine and low volume fraction of the solid particles. The advantage of single phase flow is about its simplicity and required less computational time. It should be noted that experimental, numerical and theoretical solutions are strongly affected by physical properties of nanofluids. In addition, there is some inconsistency on this subject in the literature.

The most well-known nanoparticles are Al_2O_3, CuO, TiO_2 and they are used by many researchers in their experimental works together with the base fluids of water and ethylene glycol. In spite of the different size of the particles and type of base fluids, the enhancement

☆ Communicated by W.J. Minkowycz.

* Corresponding authors.
E-mail addresses: hdemir@yildiz.edu.tr (H. Demir), somchai.won@kmutt.ac.th (S. Wongwises).

0735-1933/$ – see front matter © 2010 Elsevier Ltd. All rights reserved.
doi:10.1016/j.icheatmasstransfer.2010.12.009

Author's personal copy

Nomenclature

Cp	specific heat, J kg^{-1} K^{-1}
CFD	Computational Fluid Dynamics
d	internal tube diameter, m
h	heat transfer coefficient, W m^{-2} K^{-1}
k	thermal conductivity, W m^{-1} K^{-1}
L	length of test tube, m
m	mass flow rate, kg s^{-1}
Nu	Nusselt number
ΔP	pressure drop, Pa
Pr	Prandtl number
Re	Reynolds number
Q	heat transfer rate, W
q''	heat flux, W m^{-2}
T	temperature, °C
μ	dynamic viscosity, Pa s
ρ	density, kg m^{-3}
τ	shear stress, N m^{-2}
φ	volume fraction, %
ν	kinematic viscosity, m^2 s^{-1}

Subscripts

avg	average
bf	base fluid
exp	experimental
ext	external
f	fluid
h	hot
i	inlet
m	mean
nf	nanofluid
num	numerical
p	particle
s	surface
o	outlet
w	water

of the thermal conductivity was seen during all the experimental conditions. Firstly, Maxwell [3,4] mentioned the enhancement on the thermal conductivity of a mixture by increasing volume fraction of solid particles. Besides this, the first empirical correlations for the determination of Nusselt number for laminar and turbulent flow of a nanofluid inside a tube were developed by Pak and Cho [5] and Xuan and Li [2,6] using the mixture of water and Cu, TiO_2 and Al_2O_3 nanoparticles. A significant increase in heat transfer performance was obtained in comparison to the water for the same Reynolds number. Liu et al. [7] conducted experiments on an industrial application and studied the effects of flow rates on the slurry pressure drop and heat transfer behavior. Choi [8] investigated augmentation of heat transfer that occurred by means of nanofluids considering little or no penalty in the pressure drop. Lee et al. [9] reported increase in thermal conductivity of the nanofluid approximately 20% at the volume concentration of 4% using oxide ceramic nanofluids consisting of CuO nanoparticles having a mean diameter of 35 nm in ethylene glycol, whereas an increase up to 10% was observed using larger particles with an average diameter of 40 nm. Masuda et al. [10] reported thermal conductivity enhancement by 30% using water–Al_2O_3 nanofluid having 13 nm mean diameter particles at 4.3% volume fraction. Rea et al. [11] investigated laminar convective heat transfer and viscous pressure loss for alumina–water and zirconia–water nanofluids in a flow loop with a vertical heated tube. The heat transfer

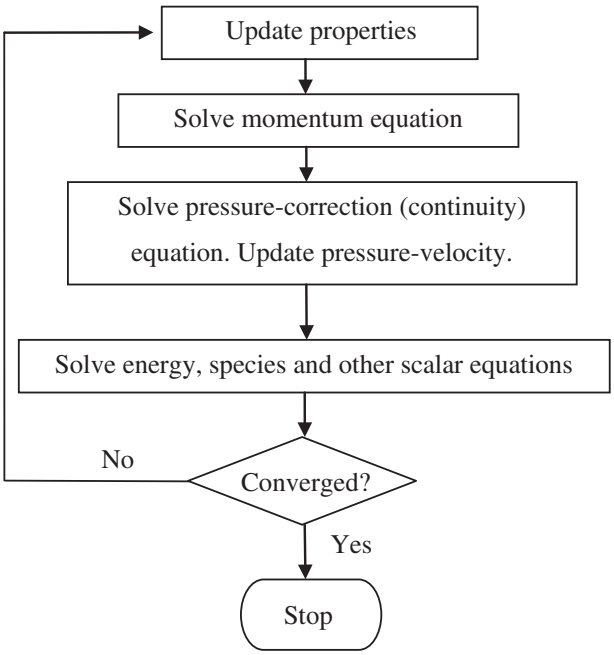


Fig. 1. Overview of the segregated method.

coefficients in the entrance region and in the fully developed region are found to be increased in 17% and 27%, respectively, for alumina–water nanofluid at 6 vol.% with respect to pure water. Bianco et al. [12] obtained heat transfer coefficient for the developing laminar forced convection flow of a water–Al_2O_3 nanofluid in a circular tube using single and two-phase models which have the maximum difference between them is about 11%. They also stated that convective heat transfer coefficient for nanofluids is greater than that of the base liquid. Heat transfer enhancement increases with the particle volume concentration, but it is accompanied by increasing wall shear stress values. Fard et al. [13] used CFD approach regarding single-phase and two-phase models to predict temperature, flow field, and calculation of heat transfer coefficient for the laminar convective heat transfer of nanofluids in a circular tube under constant wall temperature condition. Comparisons among two-phase model, single-phase model, theoretical models and experimental data were done and

Table 1
Operating conditions of the study.

Experimental study for the validation of numerical model	
Nanoparticle type, d_p	TiO_2, 21 nm
Test tube material, d, L	Copper, φ8.13 mm, 1500 mm
φ (wt.%)	0, 0.2, 0.6, 1
$T_{avg,f}$ (°C)	25–29–26.94
$T_{avg,s}$ (°C)	26.75–29.39
$T_{avg,h,w}$ (°C)	26.75–29.39
Re	4516.13–15,681.36
q'' (W m^{-2})	7233.13–13,340.99
Numerical study for the simulation of the case study	
Nanoparticle type, d_p	Al_2O_3, TiO_2, 21 nm
Test tube material, d, L	Copper, φ8 mm, 1000 m
φ (wt.%)	0, 1, 4
$T_{avg,f}$ (°C)	25.78, 28.34
$T_{avg,s}$ (°C)	26.19, 28.79
$T_{avg,h,w}$ (°C)	34.64, 36,64
Re	1000, 5000, 15,000, 25,000, 50,000, 75,000
q'' (W m^{-2})	1000, 5000, 10,000, 50,000

Author's personal copy

they reported that heat transfer coefficient clearly increases with an increase in particle concentration and two-phase model shows better agreement with experimental measurements.

Recently, Daungthongsuk and Wongwises [14] summarized the published subjects with respect to the forced convective heat transfer of the nanofluids both of experimental and numerical investigation in their review paper. Daungthongsuk and Wongwises [15] reported that thermal conductivity of nanofluids increased with increasing nanofluid temperatures and, conversely, the viscosity of nanofluids decreased with increasing temperature of nanofluids. Daungthongsuk and Wongwises [16] investigated the differences between using measured and computed thermophysical properties to describe the heat transfer performance of TiO_2–water nanofluids. Their results show that use of the models of thermo physical properties for calculating the Nusselt number of nanofluids gave similar results to use of the measured data. Daungthongsuk and Wongwises [17] presented the heat transfer coefficient and friction factor of the TiO_2–water nanofluids flowing in a horizontal double tube counter-flow

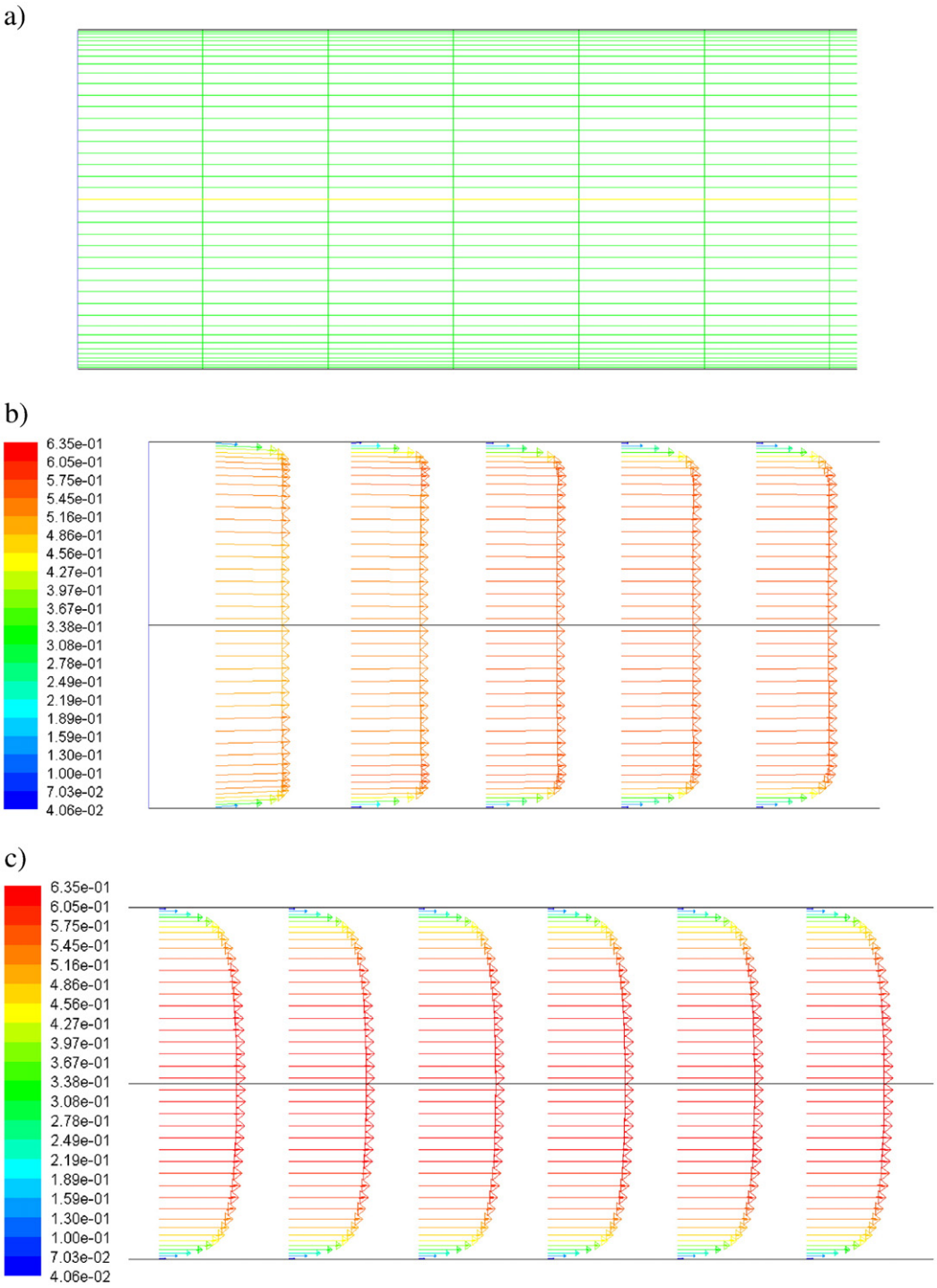


Fig. 2. Grid and velocity vectors for pure water ($Re = 4731$, $Q = 7233$ W). a) Solution grid generated in GAMBIT and used in the present analysis, axis-symmetric about *x*-axis. b) Velocity vectors at the inlet section of the test tube (m/s). c) Velocity vectors at the middle section of the test tube (m/s).

Author's personal copy

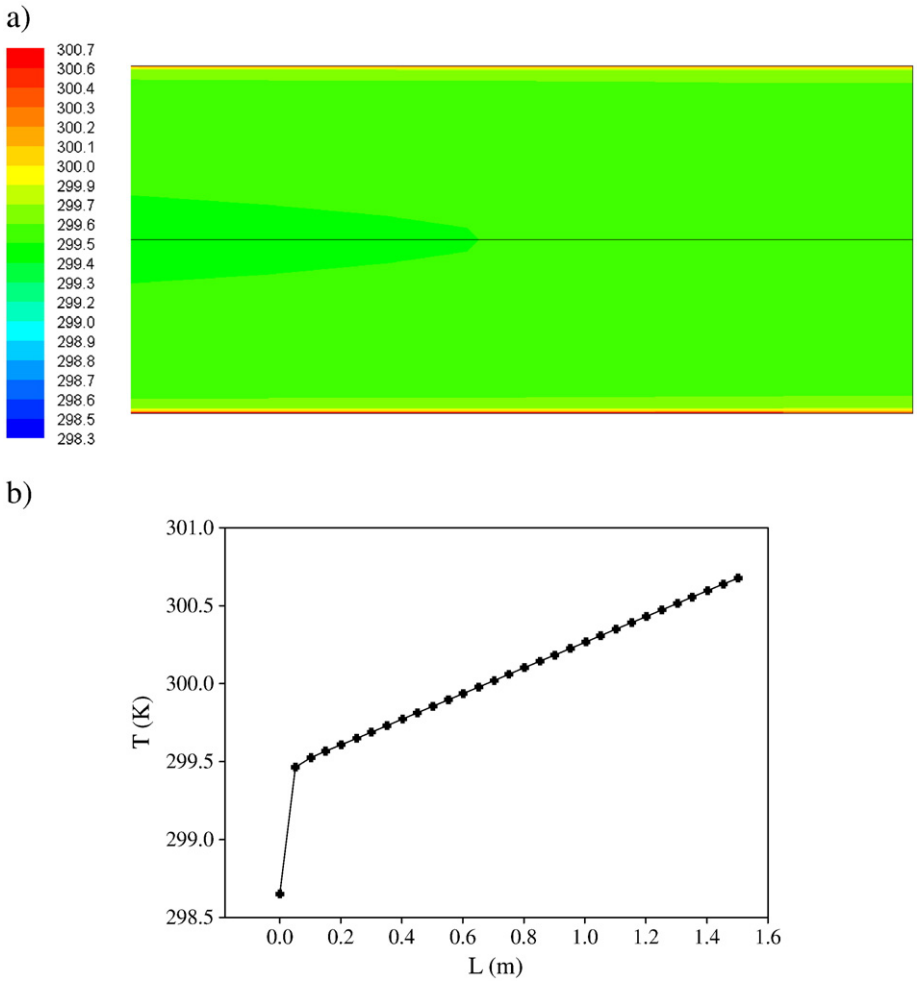


Fig. 3. Temperature distributions of outlet section and pipe surface for water and 0.6% TiO_2 nanoparticles ($Re = 14{,}880$, $Q = 11{,}862$ W). a) Temperature distribution at the outlet section of the tube. b) Surface temperature distribution along pipe.

heat exchanger under turbulent flow conditions, experimentally. Their results show that the heat transfer coefficient of nanofluid is higher than that of the base liquid and increased with increasing the Reynolds number and particle concentrations. Daungthongsuk and Wongwises [18] reported an experimental study on the forced convective heat transfer and flow characteristics of a nanofluid consisting of water and 0.2 vol.% TiO_2 nanoparticles. According to their experimental results, the heat transfer coefficient of the nanofluid increases with an increase in the mass flow rate of the hot water and nanofluid, and increases with a decrease in the nanofluid temperature, and the temperature of the heating fluid has no significant effect on the heat transfer coefficient of the nanofluid. Daungthongsuk and Wongwises [19] aimed in their paper to summarize the various models for predicting the thermophysical properties of nanofluids which have been commonly cited by a number of researchers and use them to calculate the experimental convective heat transfer coefficient of the nanofluid flowing in a double-tube counter flow heat exchanger. Daungthongsuk and Wongwises [20] summarized the published subjects with respect to the forced convective heat transfer of the nanofluids both of experimental and numerical investigation. Demir et al. [21] investigated laminar and turbulent forced convection flows of a nanofluid consisting of water and Al_2O_3 in a horizontal smooth tube with constant wall temperature numerically. Their numerical results show the heat transfer enhancement due to presence of the nanoparticles in the fluid.

Over the years, many studies have focused on the development of a model to predict the heat transfer enhancement of nanofluids. In the present work, the heat transfer behavior of a circular pipe flow has been modeled numerically in comparison to the distilled water as the base fluid with the nanofluid that is composed of distilled water and Al_2O_3 nanoparticles for a constant particle diameter and fluid temperature and various volume concentrations. Besides this, some significant experimental results reported in the study of Palm et al. [22] are used in the numerical solution. Before the modeling process in Fluent CFD program [23], validation of the model is performed using the experimental data belonging to the forced convection of nanofluids consisting of TiO_2 particles [16] regarding the comparison of calculated and measured Nusselt numbers, heat transfer coefficients and pressure drops. In addition to this, temperature distributions of inner surface and the fluids at the inlet and outlet sections of the tube, alteration of wall shear stress, Nusselt numbers, heat transfer coefficients and pressure drops with Reynolds numbers and particle concentrations, local heat transfer coefficients and pressure drops are also obtained from the numerical study and presented in the paper.

2. Sample preparation

In the present study, nanofluids provided by a commercial source (DEGUSSA, VP Disp. W740x) are used as working fluid. The detailed image of dispersed TiO_2 nanoparticles in water, taken by TEM, and

Author's personal copy

details of preparation of nanofluids can be seen from Duangthongsuk and Wongwises [16].

3. Experimental apparatus

Detailed descriptions of the experimental apparatus for studying single phase heat transfer performance of nanofluids inside a horizontal tube can be found in Duangthongsuk and Wongwises [16].

4. Data reduction

4.1. Thermal and physical properties of nanofluids

It is known that the determination of the nanofluid properties is problematic in the literature. There are also some correlations developed for this aim by Williams et al. [24]. Measurement of physical properties is performed by several researchers in the literature such as Rea et al. [11] and Duangthongsuk and Wongwises [15]. Calculation of the thermal and physical properties of the nanofluids can be done as follows:

Constant-value temperature independent densities based on nanoparticle volume fraction can be seen as follows:

$$\rho_{nf} = (1-\varphi)\rho_{bf} + \varphi\rho_p \quad (1)$$

The effective specific heat can be calculated as follows:

$$Cp_{nf} = (1-\varphi)Cp_{bf} + \varphi Cp_p \quad (2)$$

There is an alternate approach based on heat capacity concept to determine specific heat of nanofluids as follows:

$$(\rho Cp_{nf}) = (1-\varphi)(\rho Cp_{bf}) + \varphi\left(\rho Cp_p\right) \quad (3)$$

It should be noted that it is possible to have different results from Eqs. (2) and (3). Palm et al. [22] preferred to use Eq. (2) to calculate specific heat of nanofluids due to lack of experimental data on this subject.

Putra et al.'s [25] experimental data gives following equations, obtained by Palm et al.'s [22] analysis, to compute the nanofluid effective viscosity as a function of the local temperature for H_2O–Al_2O_3 nanofluid with 1% and H_2O–Al_2O_3 nanofluid with 4% respectively as follows:

$$\mu_{nf} = 2.910^{-7}T^2 - 2.10^{-4}T + 3.4.10^{-2} \quad (4)$$

$$\mu_{nf} = 3.410^{-7}T^2 - 2.310^{-4}T + 3.910^{-2} \quad (5)$$

According to the results of Palm et al.'s [22] study based on Putra et al.'s [25] experimental data, the effective thermal conductivity is determined for H_2O–Al_2O_3 nanofluid with 1% and H_2O–Al_2O_3 nanofluid with 4% respectively as follows:

$$k_{nf} = 0.003352T - 0.3708 \quad (6)$$

$$k_{nf} = 0.004961T - 0.8078 \quad (7)$$

4.2. Governing dimensionless numbers, heat flux, heat transfer coefficient and Nusselt number

In flow through ducts, the heat transfer surface surrounds and guides the stream, and the convection process is said to be internal. The velocity distribution in a duct has two distinct regions in laminar flow: first, the entrance region, where the walls are lined up by growing boundary layers, and, farther downstream, the fully developed region, where the longitudinal velocity is independent of the position along the duct. It is assumed that the duct geometry does not change with the longitudinal position. The flow through a straight duct ceases to be laminar when *Re* number exceeds approximately 2300. It is also observed that the turbulent flow becomes fully developed hydro dynamically and thermally after a relatively short entrance distance [26].

Reynolds number, Prandtl number are used in the theoretical analysis [22], the particle volume fraction (φ) and the ratios k_p/k_{bf} and

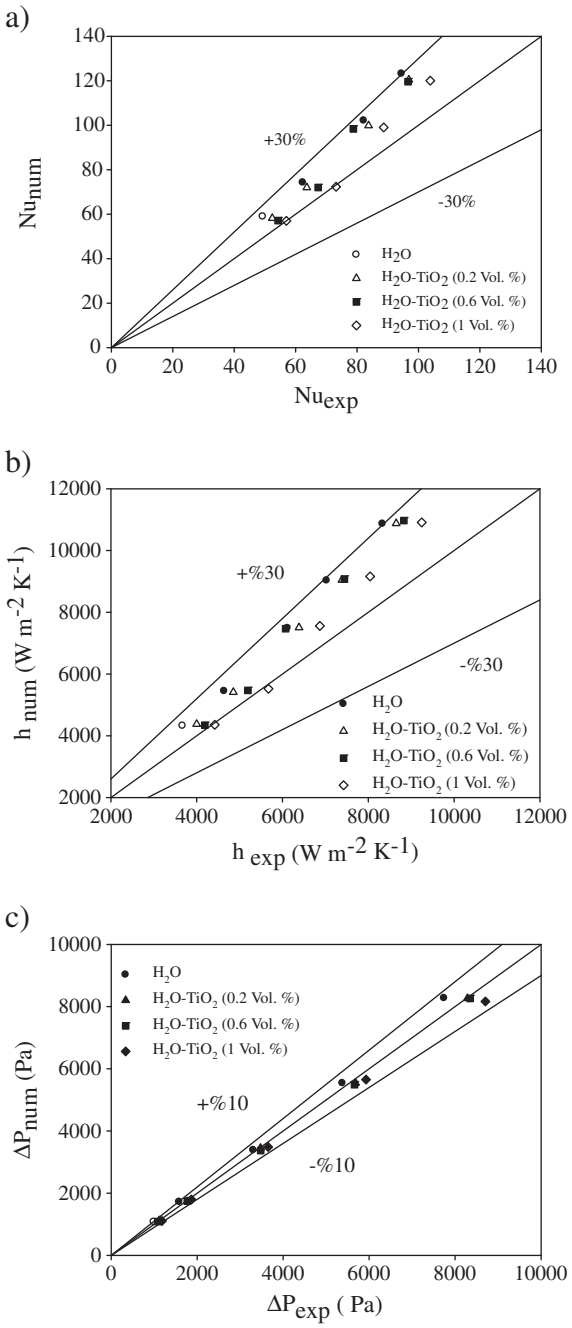


Fig. 4. Comparison of experimental and numerical Nusselt numbers, heat transfer coefficients and pressure drops using pure water with 0.2%, 0.6% and 1% TiO_2 particles data [21]. a) Experimental Nusselt numbers vs. numerical Nusselt numbers. b) Experimental heat transfer coefficient vs. numerical heat transfer coefficient. c) Experimental pressure drop vs. numerical pressure drop.

Author's personal copy

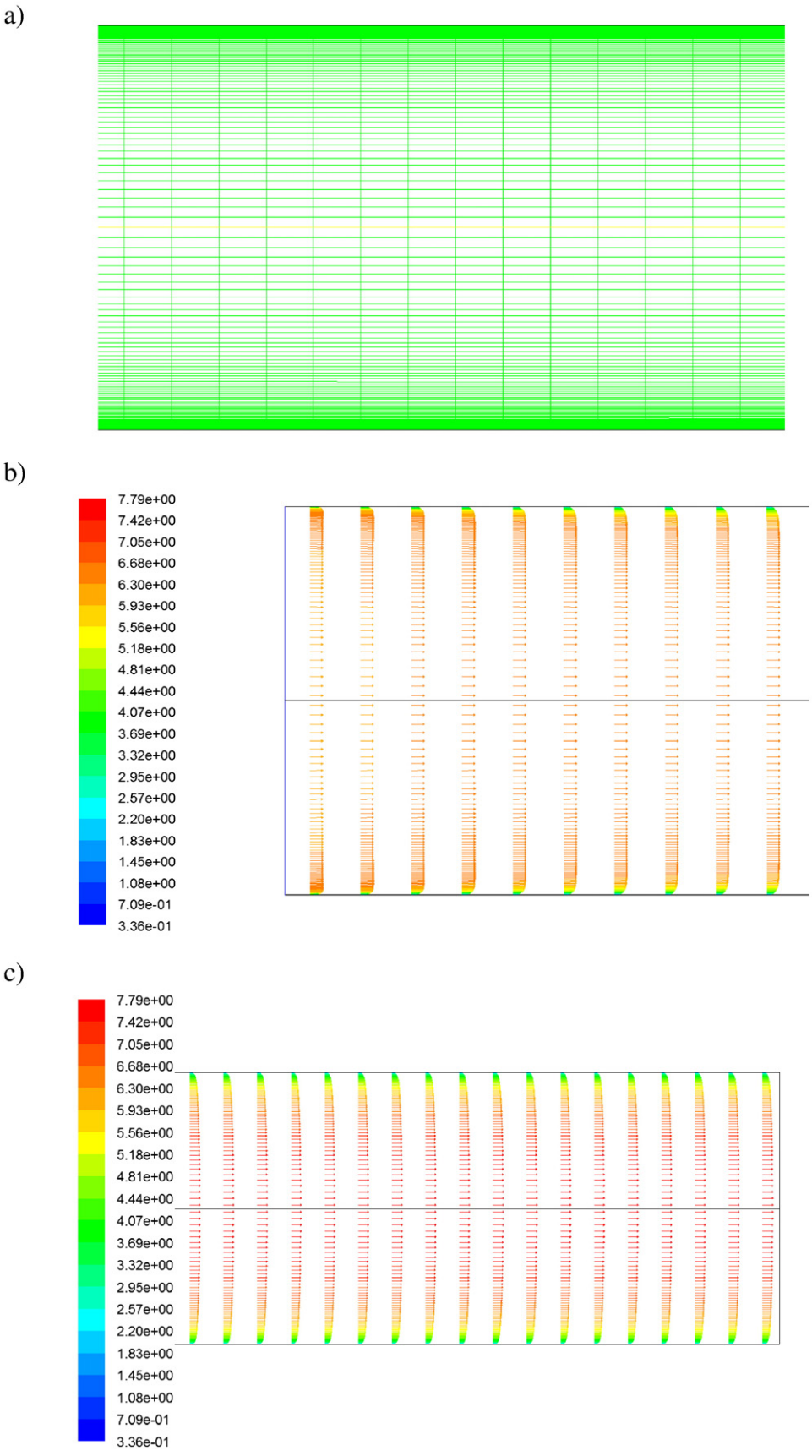


Fig. 5. Grid and velocity vectors layout obtained in the present analysis ($Re = 50{,}000$, $q'' = 10{,}000$ W m^{-2}, $T = 20$ °C). a) Solution grid generated in GAMBIT and used in the present analysis, axis-symmetric about x-axis. b) Velocity vectors at the inlet section of the test tube (m s^{-1}). c) Velocity vectors at the middle section of the test tube (m s^{-1}).

Author's personal copy

Cp_p/Cp_{bf} are used to characterize the problem and can be calculated as follows:

$$Re = \frac{2Q}{\pi d v} \tag{8}$$

$$Pr = \frac{Cp\mu}{k} \tag{9}$$

Heat flux in the test section is determined as follows:

$$q'' = \frac{m_w Cp_w (T_i - T_o)}{\pi d L} \tag{10}$$

Heat transfer coefficient of the base fluid and nanofluid can be calculated as follows:

$$h = \frac{q''}{\left(T_w - T_{f,m}\right)} \tag{11}$$

Nusselt number belongs to the base fluid and nanofluid can be calculated as follows:

$$Nu = \frac{hd}{k} \tag{12}$$

4.3. Numerical method

This problem was solved by means of the processes in Fluent CFD program [23]. FLUENT is commonly used software in CFD analysis in the literature and a detailed description of the mathematical model can be found in the Fluent User's Guide. This program uses a technique based on control volume theory to convert the governing equations to algebraic equations so they can be solved numerically. The control volume technique works by performing the integration of the governing equations about each control volume, and then generates discrimination of the equations which conserve each quantity based on control volume. The results are obtained thanks to the segregated solver algorithm shown in Fig. 1 in order to

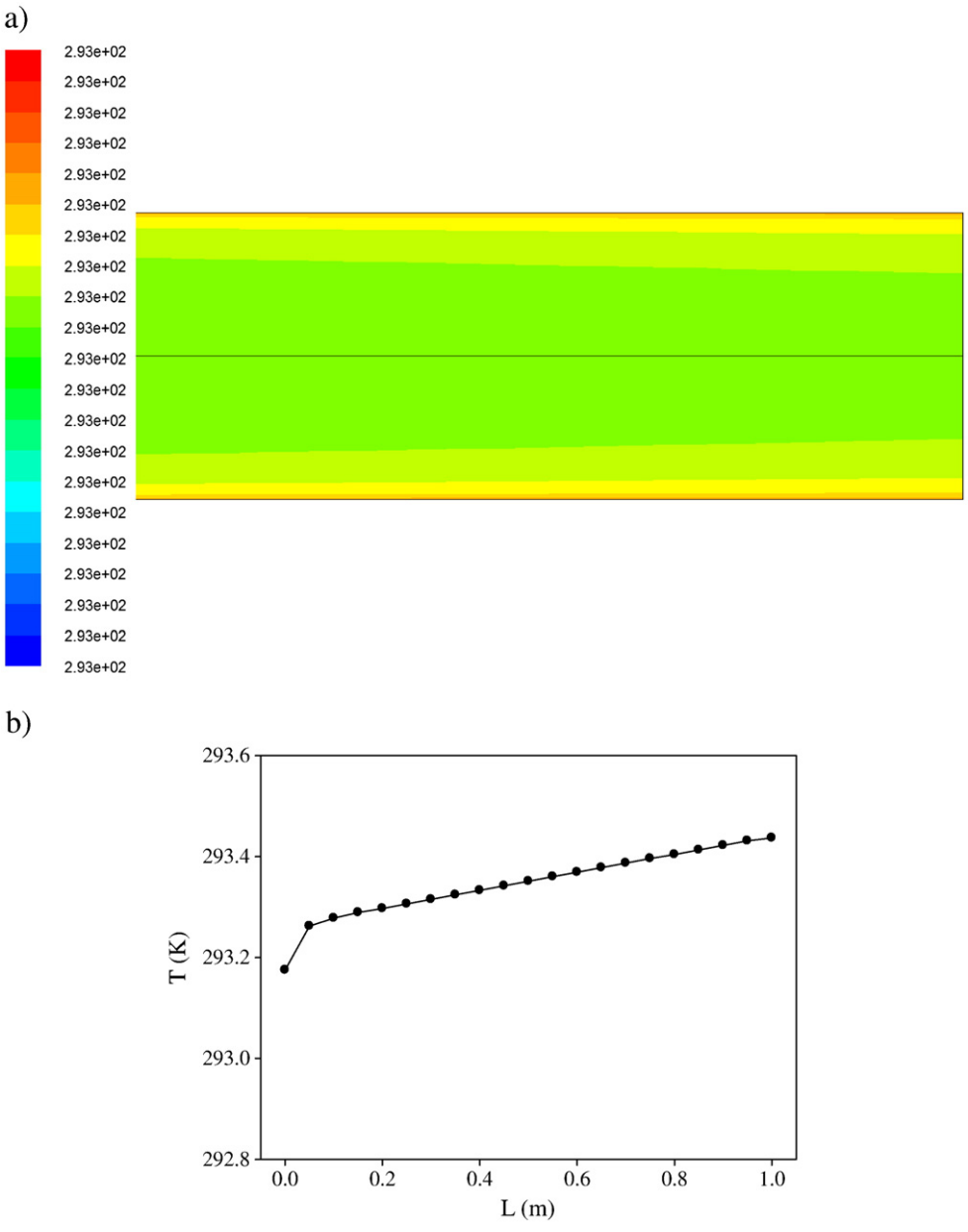


Fig. 6. Temperature distributions of inner surface and fluid in the tube ($Re = 50{,}000$, $q'' = 10{,}000\ W\ m^{-2}$, $T = 20\ °C$). a) Temperature distribution at the outlet section of the tube. b) Inner surface temperature distribution of the tube.

Author's personal copy

benefit from the experimental data reported in Palm et al.'s [22] study. According to this method the governing equations are solved sequentially, segregated one another. By means of this technique, each discrete equation is linearized implicitly respecting the equations dependent. Gambit program is used to form the model which is used for analyzing problems.

Classic single phase conservation equations were solved by control volume approach which makes possible numerical solution of governing equations by converting them to a set of algebraic equations. Governing equations have some results regarding convection terms, diffusion terms and other quantities which were discredited by second order upwind scheme. All scalar values and velocity components of the problem are calculated at the center of control volume interfaces where the grid schemes are used intensively. Semi Implicit Method for Pressure Linked Equations (SIMPLE) was used to pair the pressure and velocity. A point implicit (Gauss–Seidel) linear equation solver in conjunction with an algebraic multigrid method was used by Fluent CFD program [23] to solve the linear systems resulting from discretization schemes. Boundary conditions defined as velocity inlet at the pipe inlet and pressure outlet for the pipe exit. Turbulence intensity and hydraulic diameter defined for turbulence parameters. Constant heat flux applied to the pipe surface.

Monitor of the residuals was done during the iterative process thoroughly. All solutions were assumed to be converged when the residuals for all governing equations were lower than 10^{-6}. Optimal sizes of grid numbers were selected as 1000 (axial)×80 (radial) considering computation times and low variation with mesh size in temperature and pressure values for all conditions studied in this paper and they are placed highly near the radial flow channel entrance, as well as on all walls. Thus, it is provided that the solution became independent from the mesh size. This grid size was validated by our CFD results in all figures in the paper.

The equation for conservation of mass, or continuity equation, can be expressed as follows [23]:

$$\frac{\partial \rho}{\partial T} + \nabla\left(\rho \vec{v}\right) = S_m \tag{13}$$

Eq. (13) is the general form of the mass conservation equation and is valid for incompressible as well as compressible flows. The source S_m is the mass added to the continuous phase from the dispersed second phase and any user-defined sources.

For 2D axisymmetric geometries, the continuity equation is given by [23]

$$\frac{\partial \rho}{\partial T} + \frac{\partial}{\partial x}(\rho v_x) + \frac{\partial}{\partial r}(\rho v_r) + \frac{\rho v_r}{r}(\rho v_r) = S_m \tag{14}$$

where x is the axial coordinate, r is the radial coordinate, v_r is the radial velocity.

5. Results and discussion

A commercial software package FLUENT [23] is employed in the numerical study. It uses control volume technique to convert the governing equations to algebraic equations so they can be solved numerically. The control volume technique works by performing the integration of the governing equations about each control volume, and then generates discretization of the equations which conserve each quantity based on control volume [23]. GAMBIT was used to plot and mesh the model of the test tube. The problem under investigation is a two-dimensional (axisymmetric) steady, forced turbulent convection flow of nanofluid flowing inside a straight circular tube having diameter of 0.00813 m and a length of 1.5 m for TiO_2 and 0.008 m and 1 m for Al_2O_3. The operating conditions of the study can be seen from Table 1. The fluid enters the circular tube with uniform axial velocity and temperature. The flow and thermal fields are assumed to be axisymmetric with respect to the horizontal plane parallel to x-axis as shown in Fig. 2 for the validation study of the numerical model and Fig. 5 for the simulation study. The main frame of the grid is preferred to be intense near by the tube wall in order to investigate the alteration of boundary layer as shown in Figs. 2a and 5a.

Velocity vectors of the problems for the validation study using experimental data [16] and the simulation study using correlations of physical properties proposed by Palm et al. [22] based on the experimental data of Putra et al. [25] can be seen from Figs. 2a–b and 5a–b respectively. It should be noted that the uniformity of the flow at the inlet section of the tube and fully developed flow at the middle section of the tube can be seen from these figures respectively.

Fig. 3a for the validation study and Fig. 6a for the simulation study illustrate the temperature distribution of the flow in the outlet section of test tube. Due to the given heat flux applied to the surface of the tube, temperature values increased from center of the tube to the surface of the tube and this situation is shown in Figs. 3a and 6a. In accordance with these figures, inner surface temperature distributions of the tube can be seen from Figs. 3b and 6b for the single phase flow of the nanofluids consisting of TiO_2 particles and Al_2O_3 particles respectively.

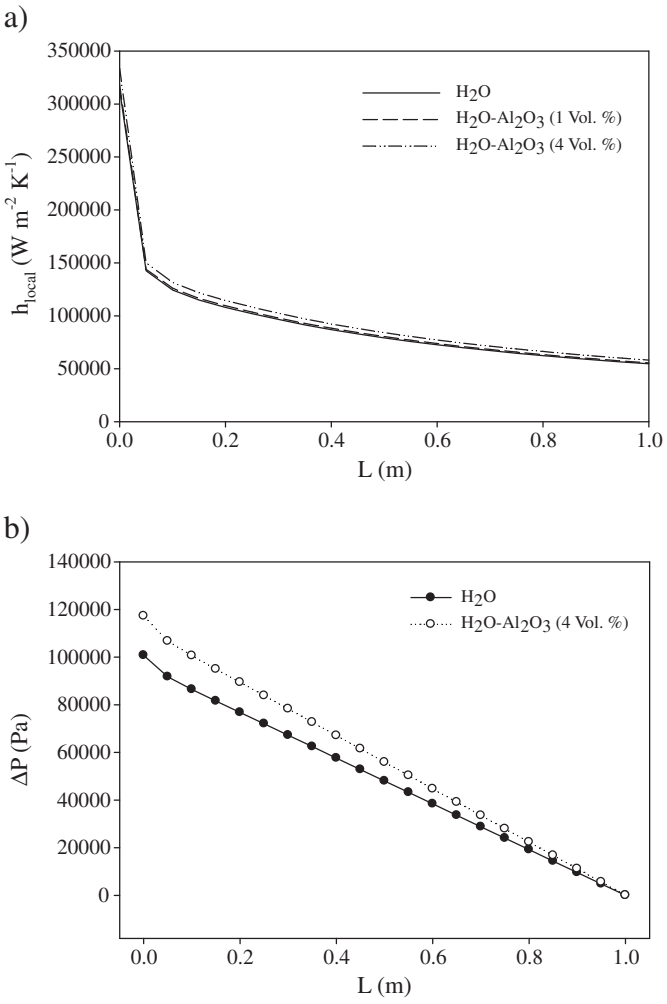


Fig. 7. Variation of local heat transfer coefficient and Pressure drop of water and nanofluid (Re = 50,000, q'' = 10,000 W, T = 20 °C, 4% concentration). a) Heat transfer coefficient—L. b) Pressure drop—L.

Author's personal copy

Validation process of numerical model is performed by means of the experimental data [16] as shown in Fig. 4 for some heat transfer characteristics of the problem. According to Fig 4, it can be clearly seen that the numerical model of Fluent [23] is in good agreement with the experimental values [16] in terms of the calculation of average Nusselt number within the range of ±30%, heat transfer coefficient within the range of ±30%, and pressure drop within the range of ±10% for the in-tube single phase flow of pure water and nanofluids with TiO_2 volume concentrations of 0.2%, 0.6% and 1%. Experimental and numerical studies are conducted for *Re* numbers between 4516 and 15681 and surface heat fluxes between 7233 and 13340 W m^{-2} (Figs. 2 and 3).

Fig. 7 shows the variation in local heat transfer coefficient and pressure drop along the length of the tube. The characteristics of the trend lines are found to be compatible with others in the literature. In addition to this, heat transfer enhancement due to nanoparticles can be seen from this figure. It is also noticed that a higher slope of relative local heat transfer coefficient can be seen at the entrance region of the tube in Fig. 7a. Fig. 7b shows the pressure drop distribution in the test tube including pure water and nanofluid with 4% Al_2O_3 concentration respectively. It can be seen from Fig. 7b that the volume concentration difference in small Reynolds numbers does not cause a significant effect, on the contrary, pressure drop increases with increasing Al_2O_3 concentration and Reynolds number in Fig. 7b.

From Fig. 8a, it is observed that wall shear stress increases with the increasing Reynolds number of the flow and also volume concentration of the nanoparticles in the tube as the mixture viscosity is increased strongly due to inclusion of nanoparticles. Fig. 8b and c displays the increase in Nusselt number, the heat transfer coefficient respectively by the various nanofluid volume concentrations over the base fluid of pure water for a fixed heat flux of 10,000 W m^{-2}. The increase in heat transfer coefficient is high for Al_2O_3, this is due to the higher Prandtl number and thermal conductivity of nanoparticles than the base fluid and also a large energy exchange process resulting from the chaotic movement of nanoparticles [27]. It should be noted that Nusselt number and heat transfer coefficient increase with increasing Reynolds number in these figures. The results complied with those obtained from Pak and Cho [5], Xuan and Li [28] and He et al. [29]. It can be seen from Fig. 8d that pressure drop increases with increasing the particle loading parameter and Reynolds number because of increasing velocity and viscosity of nanofluid.

From Fig. 9a, it is observed that wall shear stress increases with the increasing volume concentration of the nanofluid and Reynolds numbers. The shear stress has a significant increase at high Reynolds numbers. The effect of the particle concentration on the average Nusselt number and heat transfer coefficient can be clearly seen from Fig. 9b and c respectively. Nusselt number and heat transfer coefficient increase with increasing nanoparticle concentration and also Reynolds number in these figures. This shows the effect of particle concentration. It is evident that nanofluids give higher heat transfer coefficients compared to the base fluid. It can be clearly seen from Fig. 9d that there is a significant increase in pressure drop values especially at high Reynolds numbers and volume concentrations. From Fig. 9d, pressure drop increases with increasing Reynolds number and the particle loading parameter.

A large number of graphics could be generated from the output of the calculations; however, due to space limitations, only typical results are shown for limited data. It should also be noted that detailed

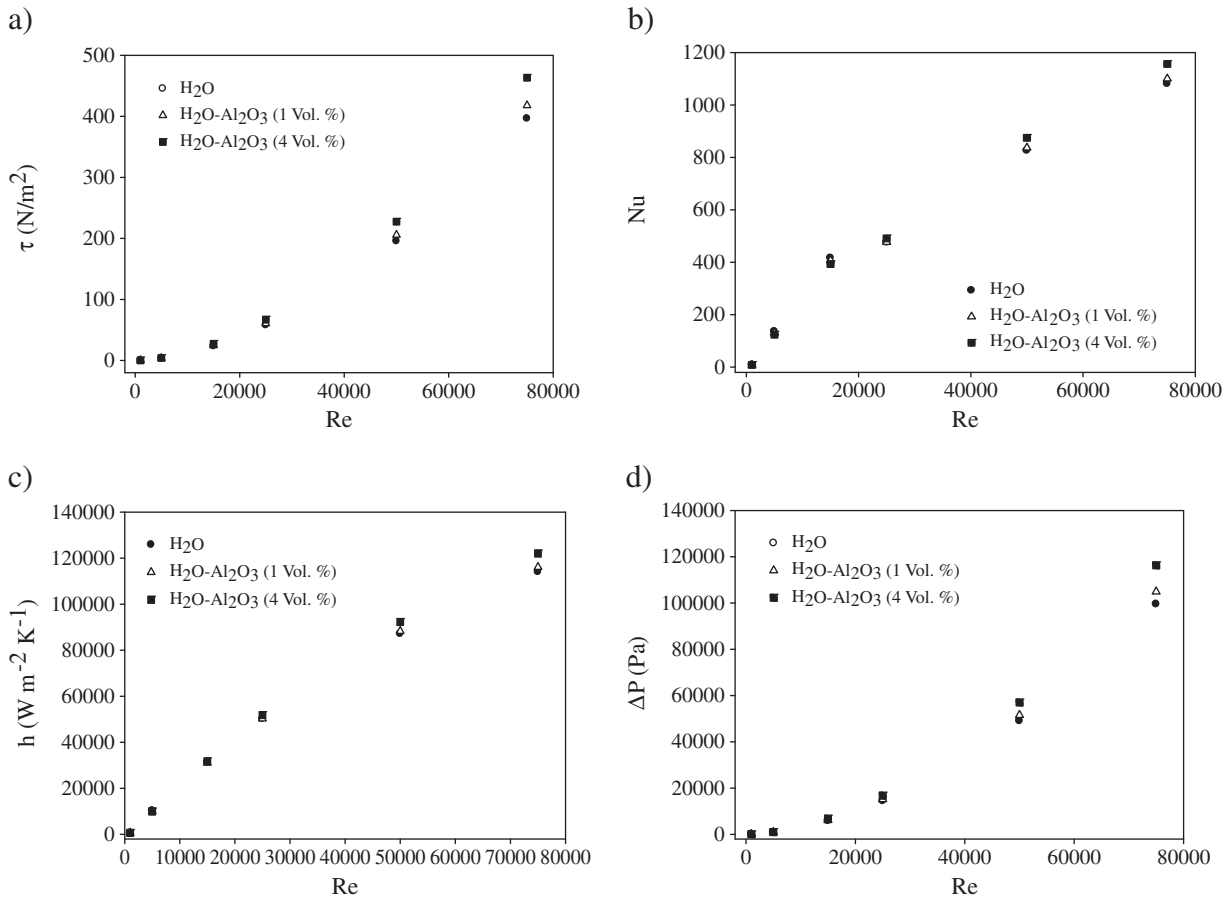


Fig. 8. Comparison of some heat transfer characteristics of different nanofluid concentrations over the base fluid of water (q'' = 10,000 W m^{-2}, T = 20 °C). a) Numerical wall shear stress vs. Re numbers. b) Numerical Nusselt numbers vs. Re numbers. c) Numerical heat transfer coefficient vs. Reynolds numbers. d) Numerical pressure drops vs. Reynolds numbers.

Author's personal copy

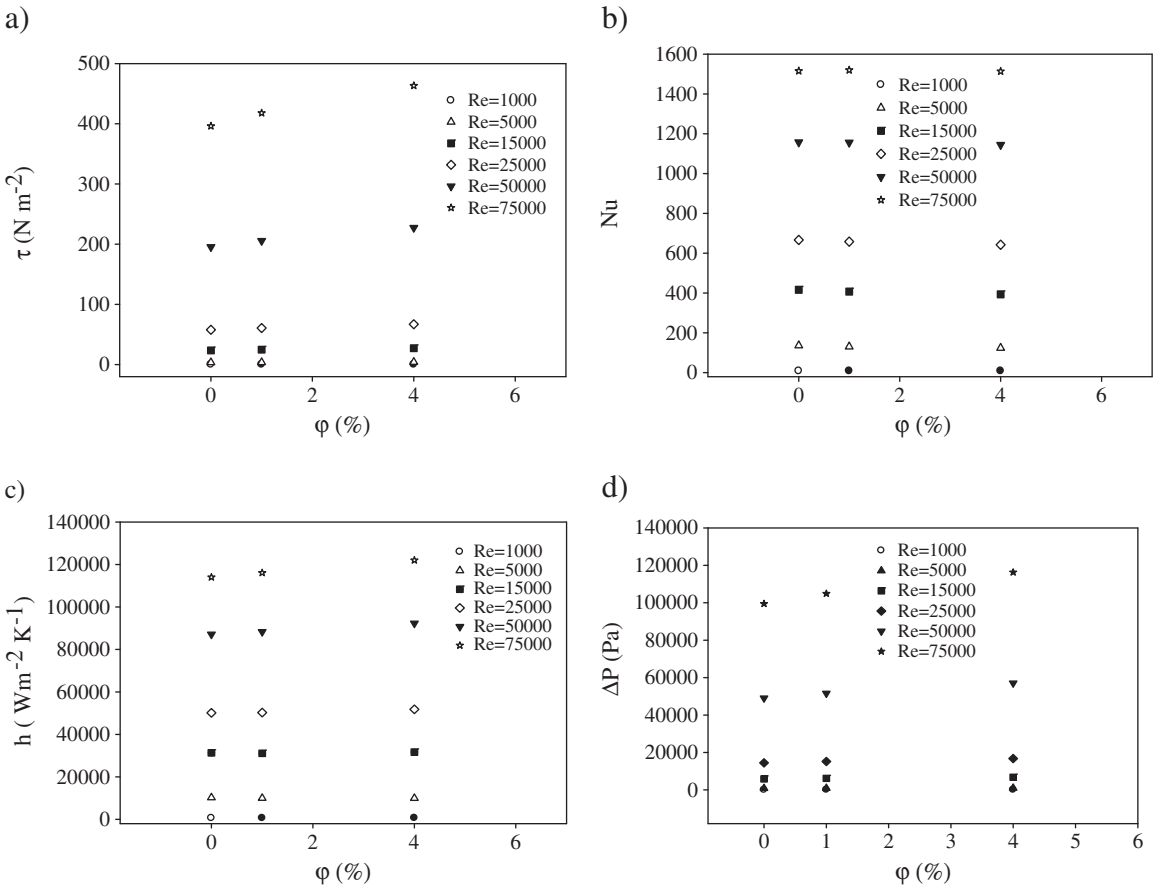


Fig. 9. Effect of particle loading φ on the some in laminar and turbulent flow ($q'' = 10{,}000\ \mathrm{W\,m^{-2}}$, $T = 20\ ^{\circ}\mathrm{C}$). a) Numerical wall shear stress vs. particle loading. b) Numerical Nusselt numbers vs. particle loading. c) Numerical heat transfer coefficient vs. particle loading. d) Numerical pressure drop vs. particle loading.

information on the explanations above and some additional figures with different experimental parameters related to this study can be seen in the authors' previous publications [14–21].

6. Conclusion

The heat transfer enhancement capabilities of nanofluids consisting of water–TiO_2 for a validation study and water–Al_2O_3 for a simulation study with various volume concentrations in a horizontal smooth tube have been investigated for forced flow conditions numerically using two dimensional governing equations.

Numerical results have clearly shown that the use of nanofluids can significantly increase heat transfer capabilities of nanofluids even for relatively small particle volume fractions.

Nanofluids with higher volume concentration have higher heat transfer enhancement and also have higher pressure drop. Therefore, judicious decision should be taken when selecting a nanofluid that will balance the heat transfer enhancement and the pressure drop penalty.

Although the nanofluid is actually a two-phase fluid in nature, the results show that the nanofluid behaves more like a pure fluid than a liquid–solid mixture.

Acknowledgments

The authors wish to thank DEGUSSA AG, Germany for the valuable donation of the nanoparticles used in the present study. The second author wishes to thank KMUTT for providing him with a Post-doctoral fellowship. The fifth author would like to thank the Thailand Research Fund, the Commission of Higher Education and the National Research University Project for providing financial support.

References

[1] U.S. Choi, Enhancing thermal conductivity of fluids with nanoparticles, ASME FED 231 (1995) 99–103.
[2] Y. Xuan, Q. Li, Heat transfer enhancement of nanofluids, Internatnal Journal of Heat Fluid Flow 21 (2000) 58–64.
[3] J.C. Maxwell, Electricity and Magnetism, Clarendon Press, Oxford, UK, 1873.
[4] J.C. Maxwell, A Treatise on Electricity and Magnetism, second ed., Oxford University Press, Cambridge, 1904, pp. 435–441.
[5] B.C. Pak, Y.I. Cho, Hydrodynamic and heat transfer study of dispersed fluids with submicron metallic oxide particles, Experimental Heat Transfer 11 (1998) 151–170.
[6] Y.M. Xuan, Q. Li, Investigation on convective heat transfer and flow features of nanofluids, Journal of Heat Transfer 125 (2003) 151–155.
[7] K.V. Liu, S.U.S. Choi, K.E. Kasza, Measurement of pressure drop and heat transfer in turbulent pipe flows of particulate slurries, Argonne National Laboratory Report, ANL-88-15, 1988.
[8] U.S. Choi, Enhancing thermal conductivity of fluid with nanoparticles, in: D.A. Singiner, H.P. Wang (Eds.), Development and Application of Non-Newtonian Flows, ASME, 231, 1995, pp. 99–105.
[9] S. Lee, S.U.S. Choi, S. Li, J.A. Eastman, Measuring thermal conductivity of fluids containing oxide nanoparticles, ASME Journal Heat Transfer 121 (1999) 280–288.
[10] H. Masuda, A. Ebata, K. Teramae, N. Hishinuma, Alteration of thermal conductivity and viscosity of liquid by dispersing ultra-fine particles (dispersions of c-Al_2O_3, SiO_2, and TiO_2 ultra-fine particles), Netsu Bussei (Japan) 4 (1993) 227–233.
[11] U. Rea, T. McKrell, L. Hu, J. Buongiorno, Laminar convective heat transfer and viscous pressure loss of alumina–water and zirconia–water nanofluids, International Journal of Heat and Mass Transfer 52 (2009) 2042–2048.
[12] V. Bianco, F. Chiacchio, O. Manca, S. Nardini, Numerical investigation of nanofluids forced convection in circular tubes, Applied Thermal Engineering 29 (2009) 3632–3642.
[13] M. H. Fard, M. N. Esfahany, M.R. Talaie, Numerical study of convective heat transfer of nanofluids in a circular tube two-phase model versus single-phase model, International Communications in Heat and Mass Transfer 37 (2010) 91–97.
[14] W. Daungthongsuk, S. Wongwises, A critical review of convective heat transfer of nanofluids, Renewable & Sustainable Energy Reviews 11 (2007) 797–817.
[15] W. Duangthongsuk, S. Wongwises, Measurement of temperature-dependent thermal conductivity and viscosity of TiO_2–water nanofluids, Experimental Thermal and Fluid Science 32 (2009) 706–714.

Author's personal copy

[16] W. Duangthongsuk, S. Wongwises, Comparison of the effects of measured and computed thermophysical properties of nanofluids on heat transfer performance, Experimental Thermal and Fluid Science 34 (2010) 616–624.
[17] W. Duangthongsuk, S. Wongwises, An experimental study on the heat transfer performance and pressure drop of TiO_2–water nanofluids flowing under a turbulent flow regime, International Journal of Heat and Mass Transfer 53 (2010) 334–344.
[18] W. Duangthongsuk, S. Wongwises, Heat transfer enhancement and pressure drop characteristics of TiO_2–water nanofluid in a double-tube counter flow heat exchanger, International Journal of Heat and Mass Transfer 52 (2009) 2059–2067.
[19] W. Duangthongsuk, S. Wongwises, Effect of thermophysical properties models on the predicting of the convective heat transfer coefficient for low concentration nanofluid, International Communications in Heat and Mass Transfer 35 (2008) 1320–1326.
[20] W. Duangthongsuk, S. Wongwises, A critical review of convective heat transfer of nanofluids, Renewable & Sustainable Energy Reviews 11 (2007) 797–817.
[21] H. Demir, A.S. Dalkilic, N.A. Kurekci, B. Kelesoglu, S. Wongwises, A numerical investigation of nanofluids forced convection flow in a horizontal smooth tube, International Heat Transfer Conference, ASME, 2010, August 8–13, USA.
[22] S.J. Palm, G. Roy, C.T. Nguyen, Heat transfer enhancement with the use of nanofluids in radial flow cooling systems considering temperature-dependent properties, Applied Thermal Engineering 26 (2006) 2209–2218.
[23] Fluent release 6.2.16, Fluent Incorporated, 2005.
[24] W.C. Williams, J. Buongiorno, L.W. Hu, Experimental investigation of turbulent convective heat transfer and pressure loss of alumina/water and zirconia/water nanoparticle colloids (nanofluids) in horizontal tubes, Journal of Heat Transfer 130 (2008) 042412.
[25] N. Putra, W. Roetzel, S.K. Das, Natural convection of nanofluids, Heat and Mass Transfer 39 (2003) 775–784.
[26] A. Bejan, G. Tsatsaronics, M. Moran, Thermal Design and Optimization, Wiley-Interscience Publication, 1996.
[27] Y. Xuan, W. Roetzel, Conceptions for heat transfer correlation of nanofluids, International Journal of Heat and Mass Transfer 43 (2000) 3701–3707.
[28] Y. Xuan, Q. Li, Investigation on convective heat transfer and flow features of nanofluids, ASME Journal of Heat Transfer 125 (2003) 151–155.
[29] Y. He, Y. Jin, H. Chen, Y. Ding, D. Cang, H. Lu, Heat transfer and flow behavior of aqueous suspensions of TiO_2 nanoparticles (nanofluids) flowing upward through a vertical pipe, International Journal of Heat and Mass Transfer 50 (2007) 2272–2281.